Performance evaluation of remote millimeter wave generation in a digital optical link incorporating a gain switched vertical cavity surface emitting laser

K. MURALI KRISHNA*, M. GANESH MADHAN
Department of Electronics Engineering, Madras Institute of Technology campus, Anna University, Chennai 600 044, India

In this work, gain switched 1.55µm Vertical Cavity Surface Emitting Laser (VCSEL) is analyzed for simultaneous transmission of Gigabit digital data as well as for remote millimeter (mm) wave generation at harmonic frequencies in a Single Mode Fiber (SMF) link. Numerical simulation of gain switching on VCSEL under square pulse excitation is carried out. For Gigabit Ethernet link transmission, the maximum link lengths for both 1.25 and 2.5Gbps are found as 106 km and 96 km at BER ≤ 10^{-10}. For a link length of 10km, the generated RF power at 2.5GHz, 5GHz and 10GHz frequencies are -25.68 dBm,-28.49 dBm and -37.13 dBm respectively, under 2.5 Gbps transmission. Signal powers of -35.05 dBm,-36 dBm, -39.52dBm and -50.56dBm are observed for 1.25GHz, 2.5GHz, 5GHz and 10GHz respectively, under 1.25Gbps transmission.

(Received April 19, 2018; accepted February 12, 2019)

Keywords: Gain switching, Full width at half maximum, VCSEL, Power spectrum, Remote mm wave generation, Radio over fiber

1. Introduction

VCSELs are cost effective laser sources which find applications in high speed communication and sensing areas. VCSEL has the potential to deliver tens of milliwatts of optical power and transfer data over single mode fiber. Using light scattering techniques, VCSEL can also measure proximity and senses reflection from nearby objects. Other emerging applications of VCSEL are highlighted elsewhere [1]. Recent research work carried out has focused on long wavelength VCSELs. Karinou et al. [2] demonstrated 28 Gbps NRZ OOK transmissions using a 1530 nm VCSEL in chromatic dispersion uncompensated SMF links. The technologies used in the authors' work are inexpensive and for optimizing the link performance, equalizers and timing recovery unit are employed. Spiga et al. [3] recorded highest modulation bandwidth of 22 GHz at 25°C for directly modulated single mode VCSELs emitting at 1.5 µm wavelength. This was achieved for a current of 6.8 mA and 9.0 mW dc power consumption. Belkin and Iakovlev [4] had compared single mode wafer fused long wavelength (LW) VCSELs and short wavelength (SW) VCSELs. They proved that LW VCSELs are superior to SW VCSELs. They are expected to find applications in Radio over Fiber (RoF) systems and optical beam forming networks for phased-array antennas. Soenen et al. [5] developed 56 Gbps PAM 4 driver IC in 130 nm SiGe BiCMOS for 1.5 µm VCSEL with an integrated 4 tap symbol spaced Feed Forward Equalization (FFE). Gatto et al. [6] experimentally demonstrated 5 GHz bandwidth in a 1580 nm VCSEL combined with direct detection after propagating through SMF. Very high capacity of 34 Gbps data rate over 100 m, 28 Gbps over 10 km and 25 Gbps over 20 km have also been achieved by employing multi carrier intensity modulation. Murali Krishna and Ganesh Madhan [7] had investigated the performance of bottom emitting 863 nm VCSEL exhibiting thermal effects with complete digital optical link for gigabit application. VCSELs can also be operated under gain switched conditions. This technique is meant for generating short optical pulses excited either electrically or optically, when the device is biased below threshold. Chen et al. [8] quantitatively analyzed a single mode 6.0 ps blue pulse, generated by gain switching from an optically injected InGaN VCSEL. Kim et al. [9] demonstrated experimentally by injecting continuous wave laser beam to a gain switched single mode 1550 nm VCSEL near the resonance wavelength to reduce pulse timing jitter. By RF gain switching a 1.55 µm VCSEL, Consoli et al. [10] produced 55 ps pulses with repetition frequencies between 1 GHz and 3 GHz. The authors also found that pulse width decreases with RF power and with the bias current until the onset of thermal effects. Valle et al. [11] observed that irregular polarization dynamics of VCSEL under sinusoidal current modulation lead to deterministic chaos. From the literature, it is found that VCSEL's are thoroughly analyzed for high data rate digital optical links at different temperatures. In the case of gain switching in VCSELs, various parameters for different diode structures were characterized. However, only few literatures report gain switching for optical microwave generation. Martin and Barry [12] demonstrated generation of highly stable 60 GHz optical mm wave signal from optical frequency comb using gain switching technique and programmable optical filter. Criado et al. [13] presented Optical Frequency Comb Generator (OFCG) design for THz photonic generation scheme using Optical Injection

Locking (OIL) and gain switching in VCSEL. Apart from gain switching and VCSEL study, Yuen and Fernando [14] numerically simulated Sub Carrier Multiplexed based architecture to support both WLAN IEEE 802.11b and WCDMA services through RoF link simultaneously. Previously, we have reported [15] a cost effective approach for transmitting Gigabit data through SMF-Free Space Optics (FSO) based hybrid link. In this present work, gain switching in a 1550 nm VCSEL is analyzed for short optical pulse generation. Further a novel idea of simultaneous data transmission and remote RF generation at the receiver is examined in a SMF link using a gain switched VCSEL transmitter. Also, magnitude of RF power generation at various harmonic frequencies of the data signal is determined at different link lengths.

2. VCSEL characteristics

A 1.55 μm single transverse mode commercial VCSEL (RayCan Co.) has been taken for the study. The device is a TO-56 pigtail VCSEL based on InAlGaAs active region and InAlGaAs/InAlAs mirrors [16]. A Spin-Flip Model (SFM) incorporating polarization properties is simplified to the standard VCSEL rate equation model (intrinsic parameters) [16], for linearly polarized single-mode operation.

Mathematically simplified, laser rate equations Eq. (1-5) considered in this work are,

$$\frac{\partial N}{\partial t} = \gamma\mu(N_{th} - N_t) - \gamma(N - N_t) - G_N(N - N_t)S \qquad (1)$$

$$\frac{\partial S}{\partial t} = \frac{\beta_{SF} N\gamma^2}{2\kappa} + 2\kappa S\left(\frac{(N - N_t)}{(N_{th} - N_t)} - 1\right) \qquad (2)$$

$$P = \frac{eS}{\tau_p F} \qquad (3)$$

$$\text{Here, } \mu = \frac{\tau_n}{\tau_e}\left(\frac{\left(\frac{I}{I_{th}} - 1\right)}{\left(1 - \frac{I}{I_{th}}\right)}\right) + 1 \qquad (4)$$

$$\text{and} \quad \kappa = \frac{1}{2\tau_p} \qquad (5)$$

'N' refers to carrier number; 'S' denotes photon number; 'P' represents optical power and 'I' denotes injection current.

Table 1 lists parameters and typical values for laser and optical fiber link.

Table 1. Parameters used for modelling VCSEL [16]and optical link [17]

Parameter	Value
VCSEL Laser diode	
Differential gain, G_N	2.152 x 10^4 s^{-1}
Differential carrier lifetime at threshold, τ_n	0.48 ns
Carrier lifetime at threshold, τ_e	1.21 ns
Photon lifetime, τ_p	19 ps
Carrier number at transparency, N_t	10.2 x 10^6
Carrier number at threshold, N_{th}	1.21 x 10^7
Threshold current, I_{th}	1.602 mA
Field decay rate, κ	26 x 10^9 s^{-1}
Decay rate of population inversion, γ	2.08 x 10^9 s^{-1}
Fraction of spontaneous emission photons coupled into laser mode, β_{SF}	6.5 x 10^{-4}
Scale factor, F	9.417 mA/mW
Electron charge, e	1.602 x10^{-19} C
Single Mode Fiber	
fiber dispersion constant, D	17 ps/nm/km
optical wavelength, λ	1550 nm
fiber attenuation factor, α_f	0.2 dB/km
velocity of light, c	3 x 10^8 m/s

These coupled laser rate equations are numerically solved using RK4 method in MATLAB to determine carrier number, photon number and optical power. For numerical simulation, the parameters for VCSEL corresponding to actual device are considered [16]. The LI curve obtained is compared with the reference [16] and shown in Fig.1. The threshold current is found as 1.6 mA and the dc curve matches well with the literature [16].

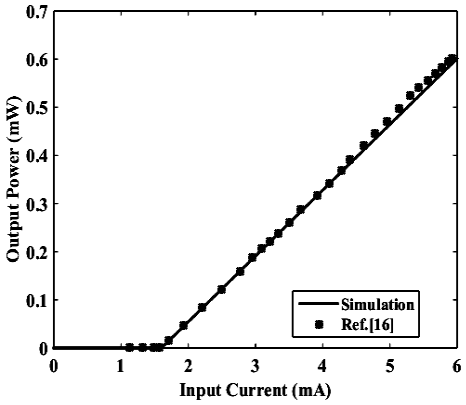

Fig. 1. L-I characteristics of VCSEL diode

The temporal responses of carrier number and laser power of the VCSEL are simulated by providing a step current with appropriate input conditions. For a step current of 6 mA given to VCSEL, the transient responses of carrier number and optical power are shown in Fig. 2(a-c). From Fig. 2 (c), it is clear that after 1.5 ns, the steady state is reached and the laser turn-on delay is roughly 0.5 ns, for the above simulation conditions.

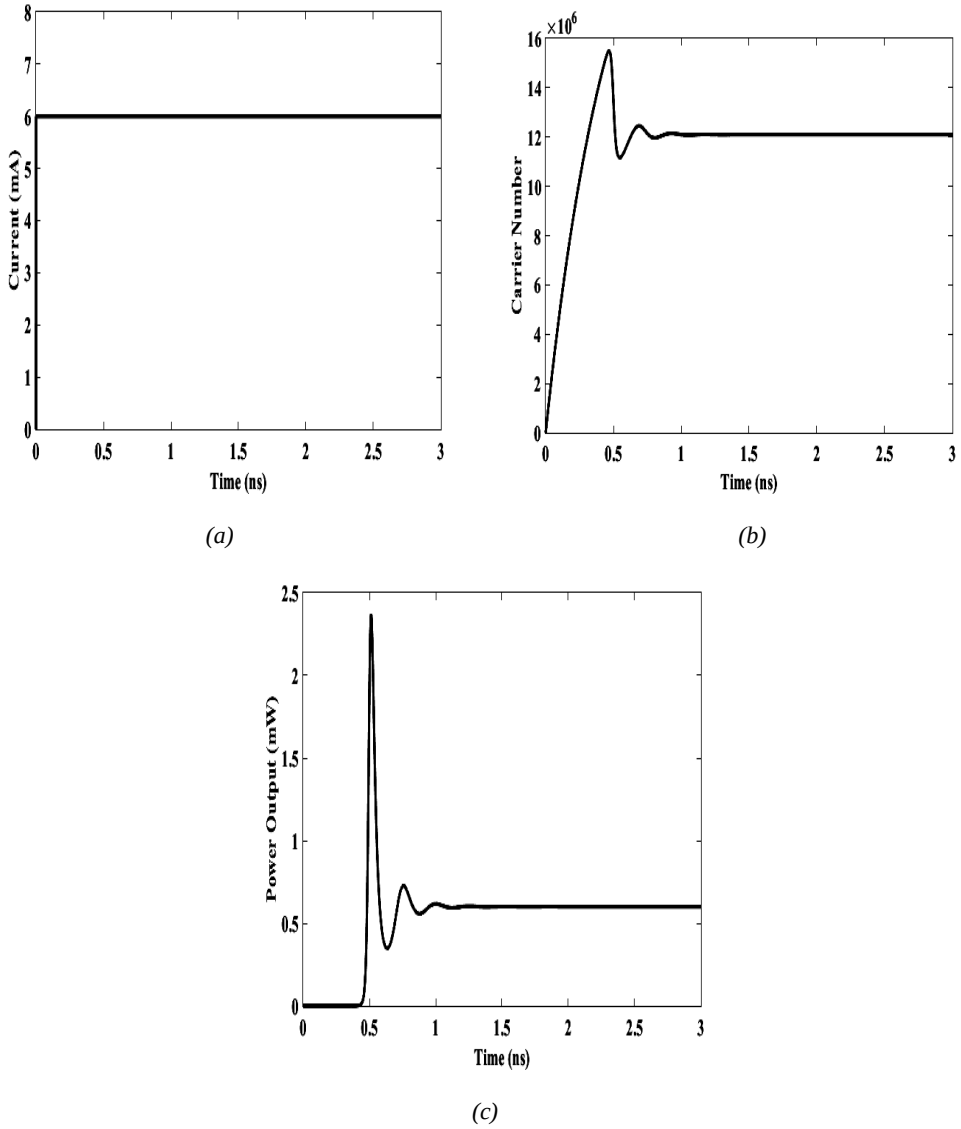

(a) *(b)*

(c)

Fig. 2. Transient characteristics of VCSEL diode at 25°C for a (a) step input current (b) Carrier Number (c) Laser Power

3. VCSEL gain switching

As, laser is biased near threshold and a sinusoidal or pulse current is provided, the laser output indicates relaxation oscillations. If the current is turned off before the onset of the second peak, a narrow pulse is generated. This is termed as gain switching in laser diodes [10]. In literature, sinusoidal RF signals were used for gain switching [10].

3.1. Sinusoidal excitation

The response of the VCSEL under sinusoidal excitation indicating gain switching is illustrated in Fig. 3(a-c). For a dc bias current of 2.45 mA along with a sinusoidal modulating current of 1.55 mA at 1.25 GHz frequency, optical pulses with FWHM of 77 ps and peak power of 1.11 mW are generated as shown in Fig. 3(d).

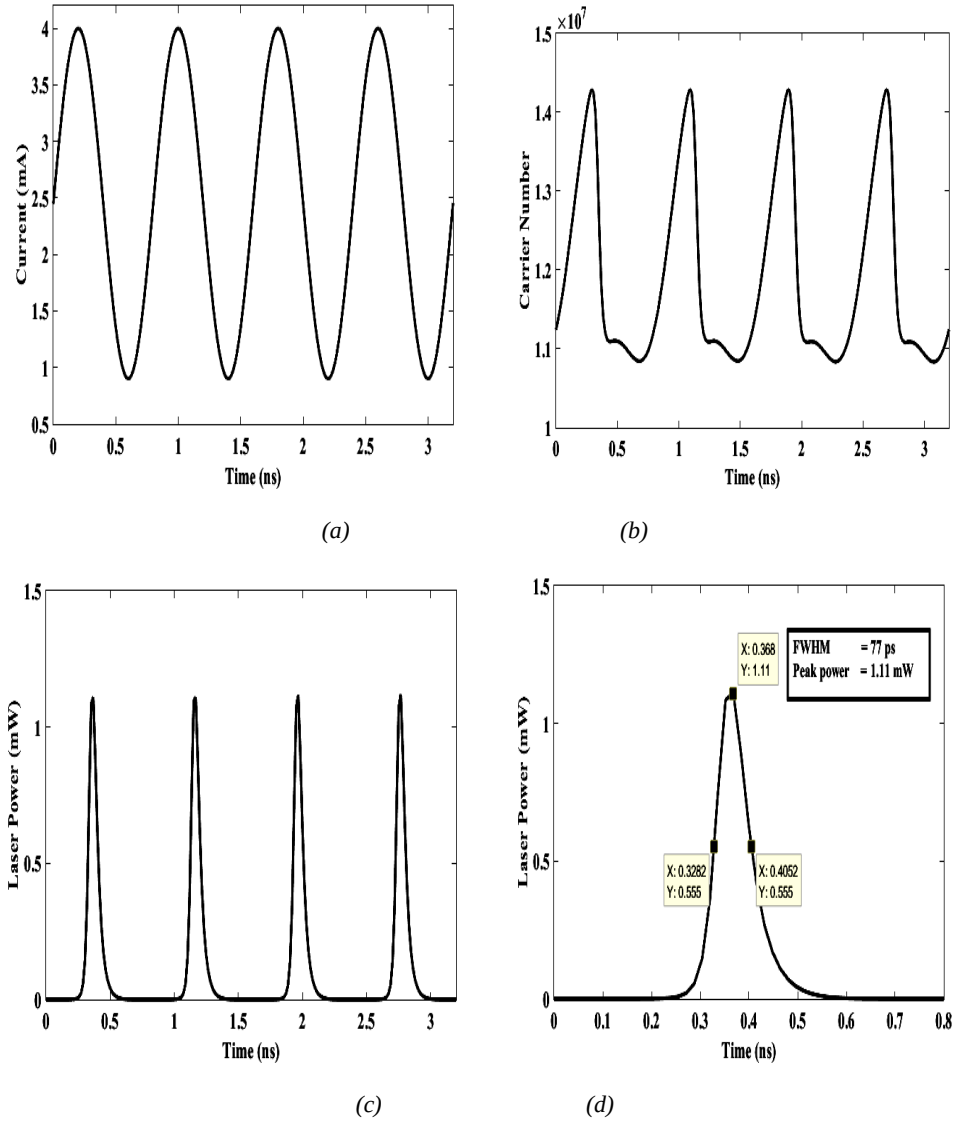

Fig. 3. Gain Switching (GS) characteristics of VCSEL diode (a) Sinusoidal current (b) Carrier Number (c) Laser Output (d) FWHM and peak power in a single pulse

3.2. Square pulse excitation

The response of the VCSEL under square pulse excitation indicating gain switching is illustrated in Fig. 4(a-c).

For a dc bias current of 0.9 mA along with a pulse amplitude of 3.1 mA with width of 0.4 ns, the optical pulses with FWHM of 68 ps and peak power of 1.337 mW are generated as shown in Fig. 4(d).

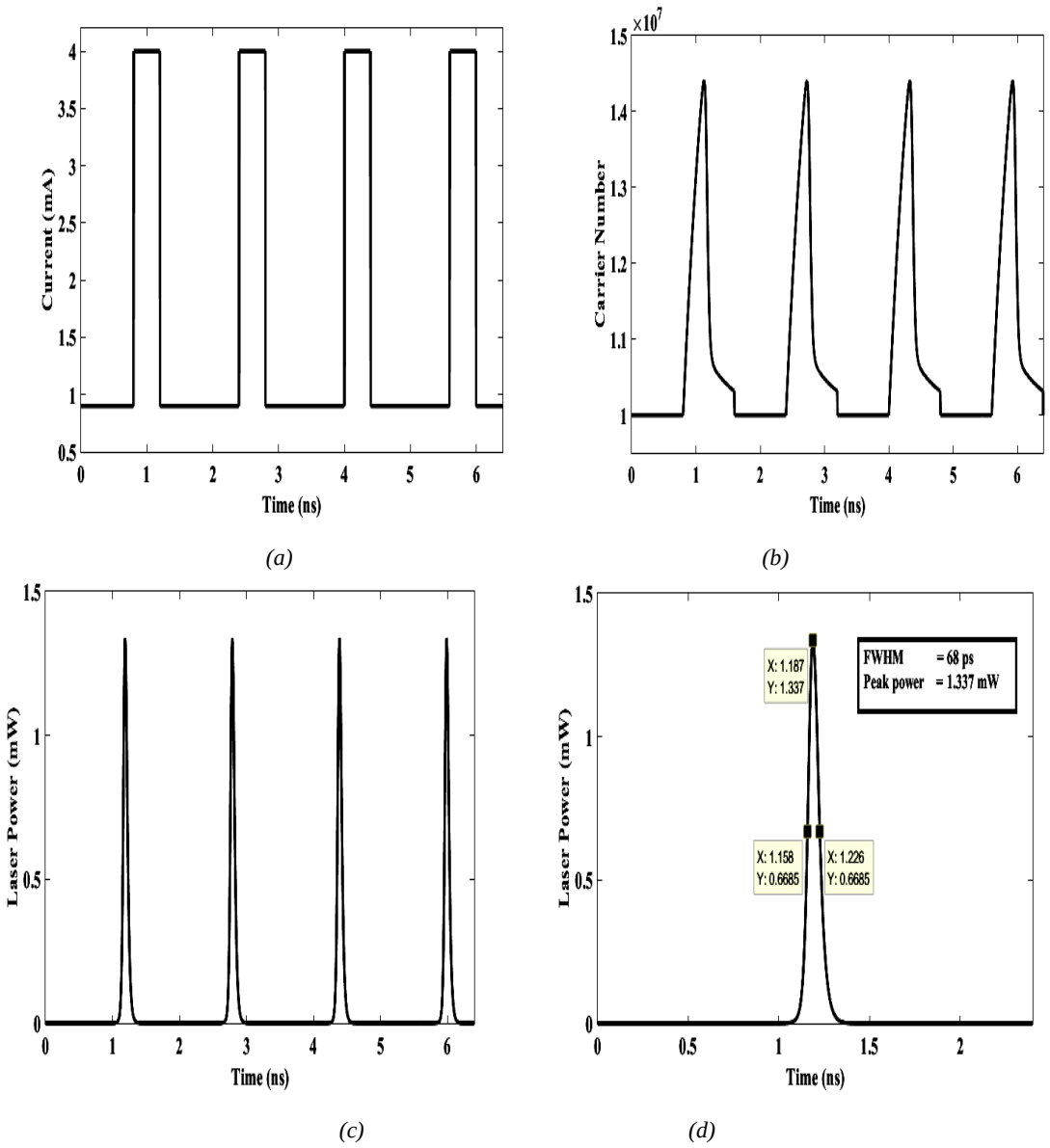

Fig. 4. Gain Switching (GS) characteristics of VCSEL diode (a) Square pulse current (b) Carrier Number (c) Laser Output (d) FWHM and peak power in a single pulse

4. Digital optical link simulation

Optical pulses spread out in time as they move along optic fiber causing bit errors. RZ pulses, with shorter pulse widths, can tolerate more dispersion than NRZ pulses. For a given average power, RZ signals have higher peak power and thus a higher signal-to-noise ratio, which yields a better BER. The schematic of optical link is shown in Fig. 5. Both the data transfer and remote mm wave generation is simultaneously realized in a single mode optical fiber link. At the receiver side, the detected signal is divided and a low pass filter provides the digital data while a band pass filter with appropriate central frequency generates the required mm waves. 1.25 Gbps and 2.5 Gbps are the data rates considered under Return to Zero (RZ) format in this work. The VCSEL transmitter is operated under gain switched mode.

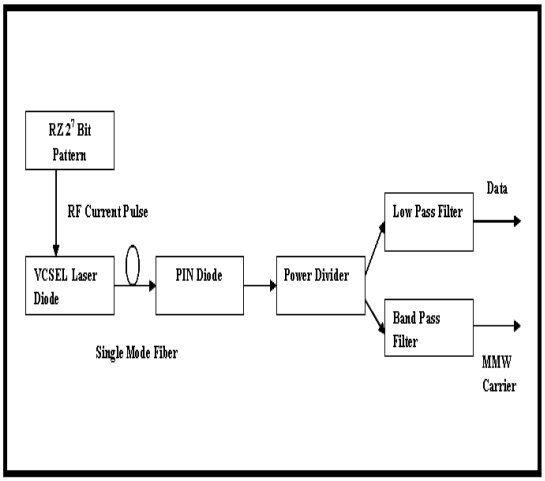

Fig. 5. Block diagram of digital optical link

4.1.1. 25 Gbps transmission

A Pseudorandom binary sequence (PRBS)-7 having a repetition period of 127 bits is considered. Hence it always returns to zero immediately after short high level pulse. RZ chosen for this simulation has 50% duty cycle and leads to less power consumption and dispersion in optical signal transmission. A current pulse of amplitude 3.1 mA, dc biased at 0.9 mA with width of 0.8 ns is applied to the VCSEL. Under these conditions, ultra short pulses of amplitude 1.337 mW at pulse width of 68 ps are observed in the output. The generated optical pulses are transmitted through a single mode optical fiber. It is observed that, at a distance of 10 km both attenuation and dispersion are not significant. The PIN detector based optical receiver is modeled as a fourth order low pass filter with cut off frequency at 75% of the data rate. The receiver comprises of a detector with responsivity of 0.75 mW/mA along with appropriate noise sources.

The received and low pass filtered signal after propagating through 10 km SMF is shown in Fig. 6 (a). The Eye diagrams evaluated for different fiber lengths namely 10 km, 100 km and 110 km, are shown in Fig.6 (b-d). This observation is similar to the literature [18]. The effect of dispersion and noise becomes significant at longer distances.

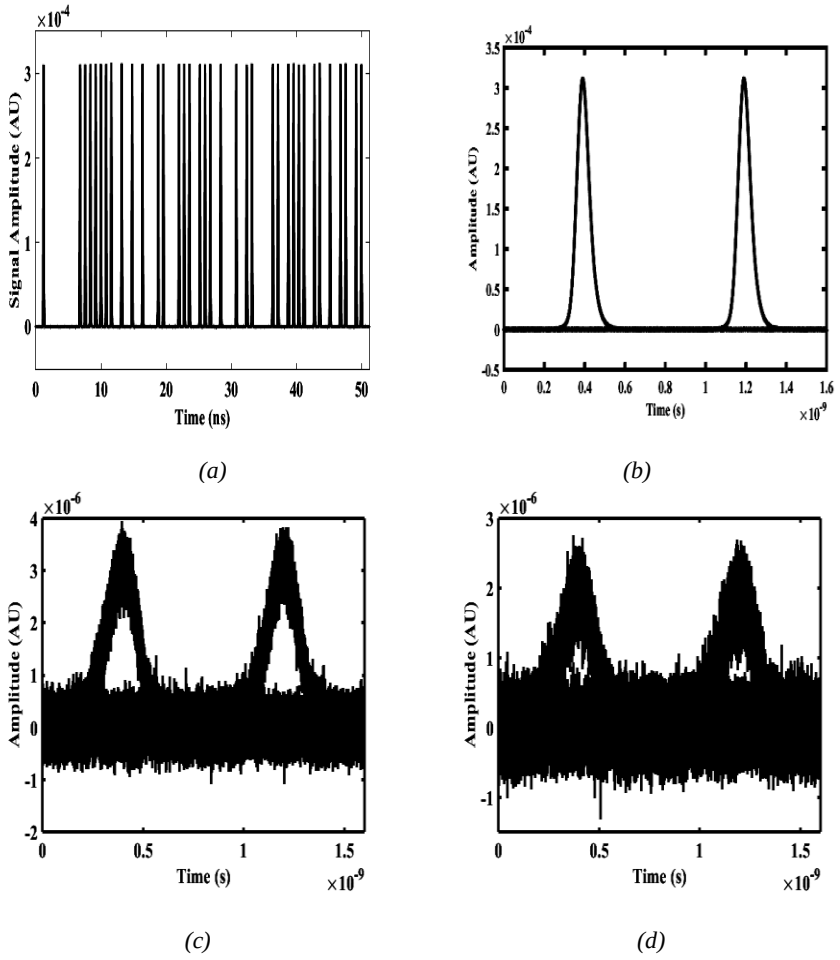

Fig. 6. (a) Received and low pass filtered signal; Eye diagram plot for (b) L = 10 km (c) L = 100 km (d) L = 110 km

The frequency contents of the signal at each block of the link are provided in Fig. 7. The 50% duty cycle RZ data spectrum shown in Fig. 7 (a) has peaks at the fundamental (1.25 GHz) and at its odd harmonics (3.75 GHz, 6.25 GHz ...) while it has nulls at its even harmonics (2.5 GHz, 5 GHz...). The RMS power spectrum is calculated using FFT technique with 2^{25} FFT points. The electrical power spectrum magnitude at fundamental (1.25 GHz) and at harmonic frequencies (2.5 GHz, 8.75 GHz and 10 GHz) are -12.51 dBm and -115.8 dBm, -29.41 dBm, -115.8 dBm respectively. After gain switching, the respective amplitudes of spectral components in laser output are -9.049 dBm, -9.533 dBm, -13.62 dBm and -16.35 dBm at 1.25 GHz, 2.5 GHz, 7.5 GHz and 10 GHz. More spectral components are observed in the optical output due to short pulses generated by gain switching.

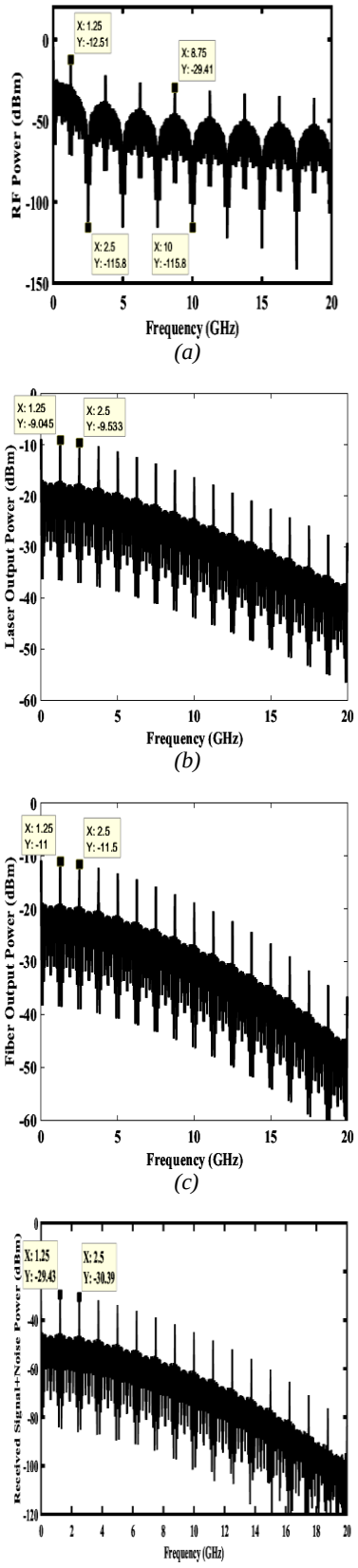

Fig. 7. Power Spectrum of (a) RZ signal (b) Laser Output Power (c) Fiber output and (d) Received RF Spectrum after PIN diode and Receiver noise sources

The fiber transfer function is given as [17] in Eq. (6),

$$H(f) = \exp\left\{ j\pi D \frac{\lambda^2}{c} L f^2 \right\} \tag{6}$$

where, L is the fiber length in km and f is the frequency in Hz.

The noise parameters used in the simulations are similar to the literature [19, 20]. The received photocurrent signal is passed through a power splitter (3 dB) and a narrow band pass filter with desired central frequencies. The generated RF carrier signal with a power of -36 dBm at 2.5 GHz is shown in Fig. 8(a,b).

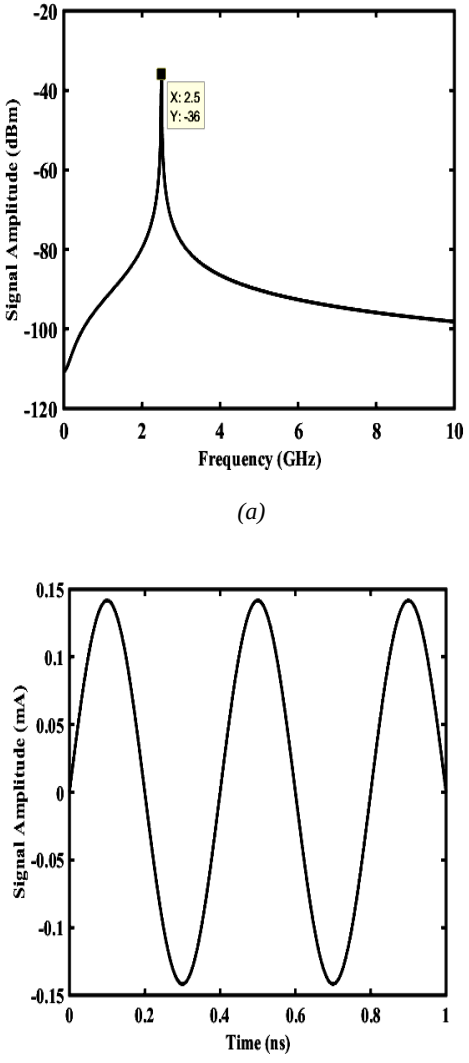

Fig. 8. (a) filtered 2.5 GHz RF signal after power splitter (b) RF signal in time domain

The simulation is repeated and the RF power obtained after band pass filtering at various fiber lengths are shown in Table 2.

Table 2. MMW generated at specific harmonics for 1.25 Gbps data signal

Fundamental RF Frequency : 1.25 GHz at -12.51 dBm					
Fiber Length (km)	Detector Current (mA)	RF Power at 1.25 GHz (dBm)	RF Power at 2.5GHz (dBm)	RF Power at 5 GHz (dBm)	RF Power at 10 GHz (dBm)
10	0.62	- 35.05	- 36.00	- 39.52	- 50.56
20	0.37	- 42.84	- 43.85	- 47.7	- 61.65
30	0.22	- 50.53	- 51.69	- 56.23	- 75.22
40	0.13	- 58.20	- 59.59	- 65.16	- 88.55
50	0.08	- 65.89	- 67.59	- 74.47	- 97.37

4.2. 2.5 Gbps transmission

The digital link simulation is repeated for 2.5 Gbps data rate. RZ pulse amplitude for 2.5 Gbps digital signal is fixed as 4 mA, dc biased at 1.4 mA. While for 1.25 Gbps pulse, the amplitude varies between 0.9 mA to 4 mA. These values are fixed based on the gain switching conditions at these data rates. Hence, laser power will be high for 2.5 Gbps, therefore RF power at receiver is slightly larger compared to 1.25 Gbps. Also the injected power into the fiber is well below Stimulated Brillouin Scattering (SBS) threshold (~5 mW) for high speed RZ pulses in long fibers (> 10 km) as pointed out [21]. This condition is satisfied in our transmission also.

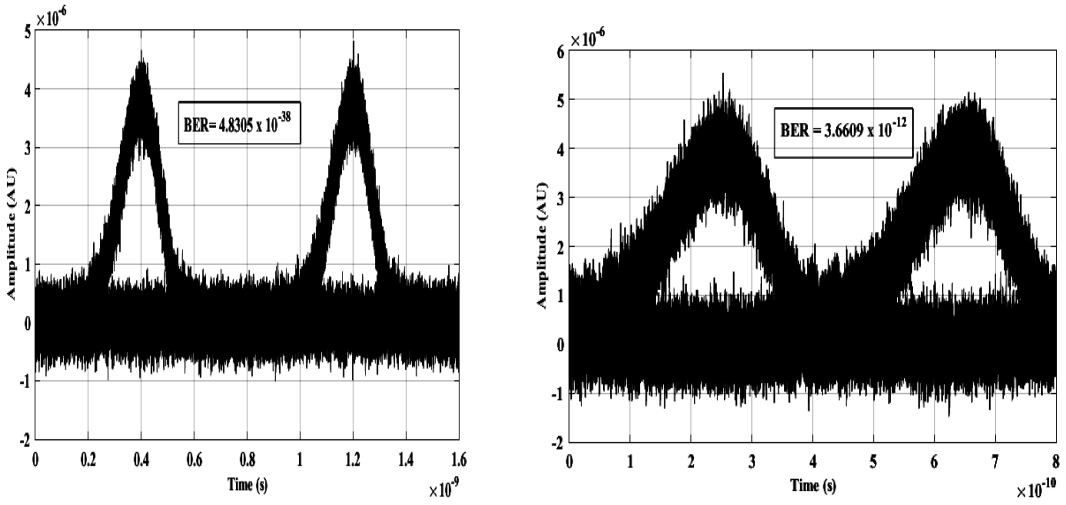

(a) *(b)*

Fig. 9. Eye diagram for a transmission Distance of 96 km for (a) 1.25 Gbps (b) 2.5 Gbps RZ data signal

Data transmitted for a longer distance of 96 km, 1.25 Gbps has less BER compared to 2.5 Gbps which are as per IEEE 802.3 z specifications for Gigabit transmission, as shown in Fig. 9(a,b). These are calculated from received eye diagrams. The simulation is repeated and the RF powers obtained after band pass filtering at various harmonic frequencies and fiber lengths for 2.5 Gbps transmission, are shown in Table 3.

Table 3. MMW generated at specific harmonics for 2.5 Gbps data signal

Fundamental RF Frequency : 2.5 GHz at -7.51 dBm				
Fiber Length (km)	Detector Current (mA)	RF Power at 2.5 GHz (dBm)	RF Power at 5 GHz (dBm)	RF Power at 10 GHz (dBm)
10	0.73	- 25.68	- 28.49	- 37.13
20	0.42	- 33.36	- 36.81	- 48.89
30	0.24	- 41.12	- 45.65	- 61.47
40	0.14	- 49.04	- 54.95	- 72.60
50	0.08	- 57.17	- 64.79	- 82.87

The performance metrics namely BER and Quality Factor are determined for entire digital optical link for data rates at 1.25 and 2.5 Gbps RZ modulated digital signals are shown in Fig. 10(a,b). Using the quality factor formula, namely $QF = (\mu_1 - \mu_0)/(\sigma_1 + \sigma_0)$, Where μ_1 and μ_0 are the mean values corresponding to levels '1' and '0' ; and σ_1 and σ_0 are the noise variances at respective levels. By substituting necessary values from eye diagram analysis for the two said data rates, we found large differences in BER values. This is evident from the fact that laser output power and receiver filter bandwidth differs proportionately for the two said data rates and this reflected in BER values.

It is understood that gain switched optical transmission under RZ coding leads to longer distance transmission for a given BER. However, the RF power generated at the receiver decreases with distances, as expected. The RF power generated for harmonics at 2.5 GHz, 5 GHz and 10 GHz during 1.25 Gbps and 2.5 Gbps transmission is illustrated in Fig. 10(c) and Fig. 10(d) respectively.

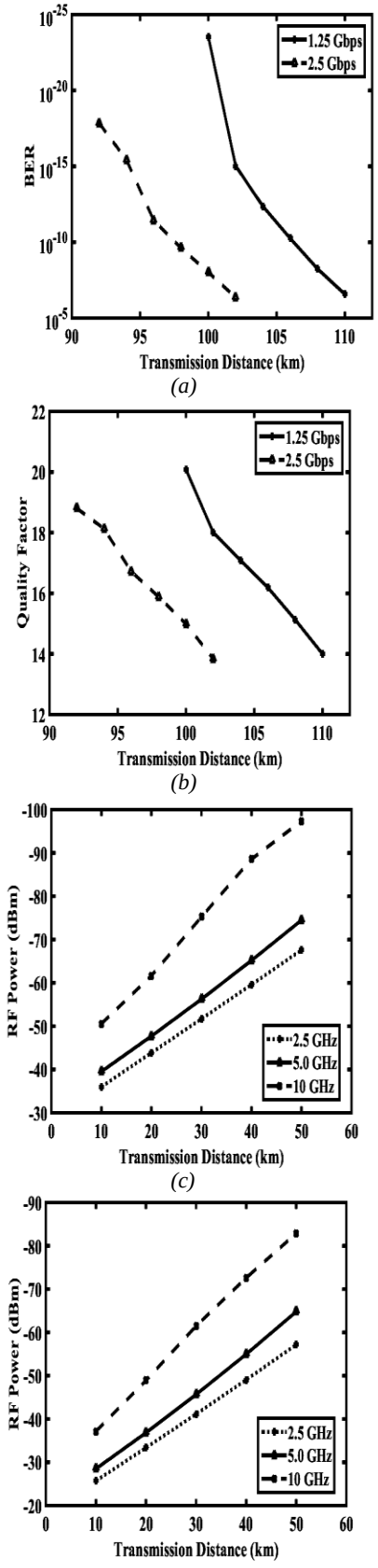

Fig.10 (a) BER Vs Transmission Distance (b) QF Vs Transmission Distance; RF Power Vs Transmission Distance for (c) 1.25 Gbps (d) 2.5 Gbps

5. Conclusions

In the present work, a cost effective approach to transmit Gigabit data and simultaneous generation of Millimeter wave carrier has been carried out. The operating data rates for the VCSEL are fixed as 1.25 Gbps and 2.5 Gbps corresponding to Ethernet standard. For a transmission distance of 20 km, corresponding to Passive Optical Network (PON) applications, the RF power is in the range of -62, -48 and -44 dBm at 10.0 GHz, 5.0 GHz and 2.5 GHz respectively at 1.25 Gbps data signal. However in the case of 2.5 Gbps transmission, the power at harmonic frequencies is slightly high. This is due to high laser output power achieved based on electrical gain switching with appropriate current pulse amplitude and 0.2 ns pulse width, data transmission. For 1.25 Gbps and 2.5 Gbps, the link lengths obtained are 106 km and 96 km respectively for a BER $\leq 10^{-10}$. This present work can be employed in High Definition Television distribution and ROF over PON network applications.

Acknowledgements

The authors gratefully acknowledge Department of Science and Technology (DST), New Delhi for providing financial support to carry out this research work under Promotion of University Research and Scientific Excellence (PURSE) II scheme. One of the authors, K. Murali Krishna is thankful to DST, New Delhi for the award of DST-PURSE fellowship.

References

[1] The Resource for VCSEL Technology: Emerging Applications, FINISAR, Available at : http://myvcsel.com/emerging-applications/ [Accessed April 19, 2018].

[2] F. Karinou, N. Stojanovic, A. Daly, C. Neumeyr, M. Ortsiefer, J. Lightwave Technol. **34**(12), 2897 (2016).

[3] S. Spiga, D. Schoke, A. Andrejew, M. Muller, G. Boehm, In: Optical fiber communication conference OFC 2016, OSA, Anaheim, California United States, 1 (2016).

[4] M. E. Belkin, V. Iakovlev, 2016 International Semiconductor Laser Conference (ISLC) 2016, IEEE, Kobe, Japan, 1 (2016).

[5] W. Soenen, R.Vaernewyck, X. Yin, S. Spiga, M. C. Amann, G.V. Steenberge, E. Mentovich, P. Bakopoulos, J. Bauwelinck, 42nd European Conference and Exhibition on Optical Communications (ECOC 2016), VDE, Dusseldorf, Germany, 1 (2016).

[6] A. Gatto, D. Argenio, P. Boffi, Opt. Express **24** (12), 12769 (2016).

[7] K. Murali Krishna, M. Ganesh Madhan, V. Nath, J. K. Mandal (eds.), Nanoelectronics, Circuits and Communication Systems 2017: Numerical simulation

of high-temperature VCSEL operation and its impact on digital optical link performance. Lecture Notes in Electrical Engineering, Springer, **511**, 337 (2018).
[8] S. Chen, A. Asahara, T. Ito, J. Zhang, B. Zhang, T. Suemoto, M. Yoshita, H. Akiyama, Opt. Express **22**(4), 4196 (2014).
[9] K. H. Kim, S. H. Lee, V. M. Deshmukh, Adv. Opt. Technol. **2012**, 1 (2012), https://dx.doi.org.10.1155/2012/247070.
[10] A. Consoli, I. Esquivias, F. J. Lopez Hernandez, J. Mulet, S. Balle, IEEE Photonic Tech. L **22**(11), 772 (2010).
[11] A. Valle, M. Sciamanna, K. Panajotov, IEEE J. Quantum Elect. **44** (2), 136 (2008).
[12] E. Martin, L. Barry, Opt. Commun. **313**, 36 (2014).
[13] A. R. Criado, C.de Dios, E. Prior, P. Acedo, M. Ortsiefer, P. Meissner, 38th International Conference on Infrared, Millimeter and Terahertz Waves (IRMMW-THz), 2013; IEEE, Mainz, Germany, 1 (2013).
[14] R. Yuen, X. N. Fernando, Wireless Pers Commun. **33**(1), 1 (2005).
[15] K. Murali Krishna, M. Ganesh Madhan, Optik **171**, 253 (2018).
[16] P. Perez, A. Valle, I. Noriega, L. Pesquera, Proc. SPIE **9134**, 1 (2014).
[17] M. M. E. Said, J. Sitch, M. I. Elmasry, J. Lightwave Technol. **23**(1), 388 (2005).
[18] L. Huo, Q. Wang, Y. Xing, C. Lou, Front. Optoelectron. **6**(1), 57 (2013).
[19] R. Yuen, X. N. Fernando, S. Krishnan, In: Canadian Conference on Electrical and Computer Engineering, 2004; IEEE, Niagara Falls, Ontario, Canada, 1715 (2004).
[20] J. Tatum (2001). VCSEL Friendly 1550 nm Specifications. Available at : http://www.ieee802.org/3/efm/public/may01/ tatum_1_0501.pdf .
[21] G. P. Agrawal, Fiber-Optic Communication Systems, Wiley, New Delhi, India, 62 (2008).

*Corresponding author: kmuralikrishnamk@gmail.com